Interference Mitigation using Delay-Doppler Channel Projection in OTFS Receivers

Sai Pradeep Muppaneni and A. Chockalingam
Department of ECE, Indian Institute of Science, Bangalore

***Abstract*—In orthogonal time frequency space (OTFS) modulation, the delay-Doppler (DD) spread in the channel causes interference across DD domain information symbols, degrading detection performance. In this paper, we propose and investigate a novel idea of DD channel projection in OTFS receivers towards the mitigation of interference due to DD channel spread. In conventional OTFS receivers, the received time domain (TD) signal is first transformed to frequency-time (FT) domain through a projection operation matched to the transmit waveform. The proposed idea in this paper is to achieve the TD to FT domain conversion without much distortion through the use of better orthonormal functions for projection. Towards this goal, the proposed receivers use projection functions that are based on DD channel knowledge. Two such receivers are proposed. The first receiver, termed as the *effective path (EP) receiver*, uses a projection function that is obtained based on an approximate characterization of the multipath channel as a channel with a single effective path, and the received signal is projected onto this effective path. A cost function is defined for this purpose, which is maximized to obtain the effective path. In the second receiver, termed as the *concatenated paths (CP) receiver*, the received signal is projected onto multiple paths and the resulting projected signals are concatenated to obtain the overall DD channel matrix. Simulation results show that the proposed EP and CP receivers offer good interference mitigation, resulting in significantly better performance compared to the conventional receiver.**

***Index Terms*—OTFS modulation, delay-Doppler domain, DD domain interference, DD channel based projection, interference mitigation.**

I. Introduction

Next generation wireless communication systems (e.g., 6G) strive to ensure reliable communication even in scenarios characterized by high mobility/Dopplers. Orthogonal time frequency space (OTFS) waveform is an attractive waveform that offers superior performance in high-Doppler channels [1]-[3]. In OTFS, at the transmitter, the information symbols are embedded in the DD domain which are converted to time domain (TD) for transmission. At the receiver, the received TD signal is converted back to DD domain where the transmitted symbols are detected. Due to delay and Doppler spreads in the channel, the received DD domain signal at the receiver experiences interference across data symbols which affects performance [4]-[7]. This interference is more pronounced in the case of fractional delays and Dopplers [8]-[10]. Our focus in this paper is to mitigate this interference to improve performance. In this regard, we note that the TD to FT domain conversion operation at the receiver can be viewed as a projection operation of the received TD signal onto a set of functions matched to the transmit waveform. We further note that the TD to FT domain conversion can be achieved without much distortion if better functions are used for the projection. In particular, if the parameters of the projection function used in the TD to FT domain conversion are chosen based on the channel's delay and Doppler spreads, it can offer the advantage of accurately recovering the symbols as such projections can mitigate the interference effects caused by the channel spreads.

Specifically, we propose two novel receivers for OTFS that use projection functions that are based on DD channel knowledge. The first proposed receiver, named as the *effective path (EP) receiver*, uses projection functions that are obtained based on an approximate characterization of the multipath channel as a channel with a single effective path, and the received signal is projected onto this effective path. A cost function is defined for this purpose, which is maximized to obtain the effective path. The effective path is so chosen to reduce interference by making the DD channel matrix close to the identity matrix, which is the ideal desired channel matrix. The idea in the second proposed receiver, named as the *concatenated paths (CP) receiver*, is to use multiple paths for the projection, potentially getting complementary views of the same underlying signal and use these projections for obtaining the DD signal for detection. Accordingly, the received signal is projected onto multiple paths and the resulting projected signals are concatenated to obtain the overall DD channel matrix. We evaluate the bit error performance of the proposed receivers in comparison with that of the conventional receiver, by considering minimum mean square error (MMSE) detection. In addition, we consider an iterative soft interference cancellation based detection and assess the closeness of the performance of the proposed receivers with a lower bound on the performance of the optimum maximum likelihood (ML) detection. The proposed EP and CP receivers are shown to offer good interference mitigation, resulting in significantly better performance compared to the conventional receiver. Also, the proposed receivers along with the iterative soft interference cancellation based detection achieve close to the lower bound on the optimum detection performance within about a dB at high signal-to-noise ratios (SNRs).

II. OTFS system model

At the OTFS transmitter, MN information symbols are multiplexed in the DD domain to obtain an $M \times N$ symbol matrix $\mathbf{X}_{\rm DD} \in \mathbb{A}^{M \times N}$, where $\mathbb{A}$ is the modulation alphabet from which the information symbols are drawn. M and N denote the number of bins along the delay and Doppler

This work was supported in part by the J. C. Bose National Fellowship, Department of Science and Technology, Government of India.

domains, respectively. The widths of the delay and Doppler bins are T/M and $\Delta f/N$, respectively, where $\Delta f = 1/T$, and $B = M\Delta f$ and NT are the bandwidth and time duration of transmission, respectively. The symbols in the DD domain are converted to FT domain using inverse symplectic finite Fourier transform (ISFFT), i.e., the DD domain symbol martix $\mathbf{X}_{\rm DD}$ is converted to an FT domain matrix $\mathbf{X}_{\rm FT} \in \mathbb{C}^{M\times N}$ as

$$\mathbf{X}_{\rm FT} = \mathbf{F}_M \mathbf{X}_{\rm DD} \mathbf{F}_N^H, \tag{1}$$

where $\mathbf{F}_M$ is the unitary discrete Fourier transform (DFT) matrix of size M. The $\mathbf{X}_{\rm FT}$ matrix is then converted into a continuous time domain signal using Heisenberg transform as

$$x(t) = \sum_{m=0}^{M-1}\sum_{n=0}^{N-1} \mathbf{X}_{\rm FT}[m,n] g(t-nT) e^{j2\pi m\Delta f(t-nT)}, \tag{2}$$

where $g(t)$ is the transmit pulse. The above FT domain to time domain conversion operation can be viewed as using a set of MN orthonormal functions

$$\{\phi_{m,n,0,0}(t) : m \in \{0,\cdots,M-1\}, n \in \{0,\cdots,N-1\}\} \tag{3}$$

for converting $\mathbf{X}_{\rm FT}$ into the continuous time domain signal as

$$x(t) = \sum_{m=0}^{M-1}\sum_{n=0}^{N-1} \mathbf{X}_{\rm FT}[m,n]\ \phi_{m,n,0,0}(t), \tag{4}$$

where the (m,n)th orthonormal function $\phi_{m,n,\tau,\nu}(t)$ is

$$\phi_{m,n,\tau,\nu}(t) = g(t-nT-\tau)e^{j2\pi m\Delta f(t-nT-\tau)}e^{j2\pi\nu(t-\tau)}. \tag{5}$$

The time domain signal $x(t)$ is passed through a doubly-selective channel, which is considered to have P paths in the DD domain, where the ith path has delay τ_i, Doppler shift ν_i, and fade coefficient h_i, and the channel response is represented in the DD domain as $h(\tau,\nu) = \sum_{i=1}^{P} h_i \delta(\tau-\tau_i)\delta(\nu-\nu_i)$, where τ_is and ν_is are assumed to take fractional values. The received time domain signal $y(t)$ is given by

$$y(t) = \sum_{i=1}^{P} h_i x(t-\tau_i) e^{j2\pi\nu_i(t-\tau_i)} + w(t), \tag{6}$$

where $w(t)$ is the additive white Gaussian noise (AWGN). To recover the DD domain information symbols from $y(t)$, the approach involves first obtaining the FT domain signal from $y(t)$ and transforming it back to the DD domain for symbol detection. The time domain to FT domain conversion is done through Wigner transform as

$$\mathbf{Y}_{\rm FT}[m,n] = A_{g,y}(f,t)\big|_{f=m\Delta f, t=nT}, \tag{7}$$

where the ambiguity function $A_{g,y}(f,t)$ is given by

$$A_{g,y}(f,t) = \int g^*(t'-t)y(t)e^{-j2\pi f(t'-t)}dt'. \tag{8}$$

From (2), (4), we note that (6) can be written as

$$y(t) = \sum_{i=1}^{P} h_i \sum_{m=0}^{M-1}\sum_{n=0}^{N-1} \mathbf{X}_{\rm FT}[m,n]\phi_{m,n,\tau_i,\nu_i}(t) + w(t), \tag{9}$$

i.e., the effect of each path of the received signal can be written as the linear combination of MN orthonormal functions (different set of orthonormal functions for different paths). Therefore, (7) can be written as

$$\mathbf{Y}_{\rm FT}[m',n'] = \langle y(t), \phi_{m',n',\tau,\nu}(t)\rangle\big|_{\tau=0,\nu=0}, \tag{10}$$

where $\langle a(t), b(t)\rangle$ denotes the inner product of signals $a(t)$ and $b(t)$, i.e., $\langle a(t), b(t)\rangle = \int_{-\infty}^{\infty} a(t)b^*(t)dt$. Now, the input-output relation between $\mathbf{y}_{\rm FT} \triangleq {\rm vec}(\mathbf{Y}_{\rm FT})$ and $\mathbf{x}_{\rm FT} \triangleq {\rm vec}(\mathbf{X}_{\rm FT})$ can be written in vector form as

$$\mathbf{y}_{\rm FT} = \sum_{i=1}^{P} h_i \mathbf{H}_{\rm FT}^{(i)} \mathbf{x}_{\rm FT} + \tilde{\mathbf{w}} = \mathbf{H}_{\rm FT}\mathbf{x}_{\rm FT} + \tilde{\mathbf{w}}, \tag{11}$$

where $\mathbf{H}_{\rm FT}^{(i)} \in \mathbb{C}^{MN\times MN}$ with $\mathbf{H}_{\rm FT}^{(i)}[n'M+m', nM+m] = \langle \phi_{m,n,\tau_i,\nu_i}(t), \phi_{m',n',\tau,\nu}(t)\rangle\big|_{\tau=0,\nu=0}$ and $\mathbf{H}_{\rm FT} = \sum_{i=1}^{P} h_i \mathbf{H}_{\rm FT}^{(i)}$, and the elements of $\tilde{\mathbf{w}}$ are the projections of AWGN onto the set of orthonormal functions. Upon obtaining $\mathbf{Y}_{\rm FT}$, the corresponding DD domain matrix $\mathbf{Y}_{\rm DD}$ is obtained by applying symplectic finite Fourier transform (SFFT) as

$$\mathbf{Y}_{\rm DD} = \mathbf{F}_M^H \mathbf{Y}_{\rm FT} \mathbf{F}_N, \tag{12}$$

and the end-to-end relation between $\mathbf{x}_{\rm DD} \triangleq {\rm vec}(\mathbf{X}_{\rm DD})$ and $\mathbf{y}_{\rm DD} \triangleq {\rm vec}(\mathbf{Y}_{\rm DD})$ can be written as (using the property ${\rm vec}(\mathbf{ACB}) = (\mathbf{B}^T \otimes \mathbf{A}){\rm vec}(\mathbf{C})$ [11])

$$\begin{aligned}\mathbf{y}_{\rm DD} &= \left(\mathbf{F}_N \otimes \mathbf{F}_M^H\right)\mathbf{H}_{\rm FT}\left(\mathbf{F}_N^H \otimes \mathbf{F}_M\right)\mathbf{x}_{\rm DD} + \mathbf{w} \\ &= \mathbf{H}_{\rm DD}\mathbf{x}_{\rm DD} + \mathbf{w},\end{aligned} \tag{13}$$

where $\mathbf{H}_{\rm DD} = \left(\mathbf{F}_N \otimes \mathbf{F}_M^H\right)\mathbf{H}_{\rm FT}\left(\mathbf{F}_N^H \otimes \mathbf{F}_M\right)$ is the DD domain channel matrix, and $\mathbf{w} = (\mathbf{F}_N \otimes \mathbf{F}_M^H)\tilde{\mathbf{w}}$ is the DD domain noise vector. Since the components of $\tilde{\mathbf{w}}$ are the projections of AWGN onto a set of orthonormal functions, the components of $\tilde{\mathbf{w}}$ are i.i.d Gaussian. Further, as $\tilde{\mathbf{w}}$ is converted to $\mathbf{w}$ through an orthonormal operation $(\mathbf{F}_N \otimes \mathbf{F}_M^H)\tilde{\mathbf{w}}$, the components of $\mathbf{w}$ are also i.i.d Gaussian. Detection algorithms can be applied on the vectorized DD domain system model in (13) to obtain the decoded information symbols.

III. Proposed DD channel projection based receivers

In this section, we introduce the proposed DD channel projection and two receivers based on this projection. In conventional OTFS receivers, the FT domain matrix $\mathbf{Y}_{\rm FT}$ is obtained through the projection of $y(t)$ onto the set of orthonormal functions $\{\phi_{m',n',\tau,\nu}(t)\}$ at $\tau = \nu = 0$ (see Eqn. (10)). This choice of $\tau = \nu = 0$ in $\{\phi_{m',n',\tau,\nu}(t)\}$ for the projection implies that $y(t)$ is matched to the waveform on the transmit side (see Eqn. (7)). The choice of τ and ν parameters in the projection function $\{\phi_{m',n',\tau,\nu}(t)\}$ can influence the retrieval of DD domain symbols. In particular, when these parameters are chosen based on the channel's delay and Doppler spreads, it can offer advantages of accurately recovering the symbols as such projections can mitigate the interference effects caused by the channel spreads. Motivated by this, we consider receivers that use projections with $\tau \neq 0$,

$\nu \neq 0$ in $\{\phi_{m',n',\tau,\nu}(t)\}$, chosen based on DD channel knowledge. In this case, $\mathbf{Y}_{\rm FT}[m',n']$ can be expressed as

$$\begin{aligned}\mathbf{Y}_{\rm FT}[m',n'] &= \langle y(t), \phi_{m',n',\tau,\nu}(t)\rangle \\ &= \sum_{i=1}^{P} h_i \sum_{m=0}^{M-1}\sum_{n=0}^{N-1} \mathbf{X}_{\rm FT}[m,n]\, \langle \phi_{m,n,\tau_i,\nu_i}(t), \phi_{m',n',\tau,\nu}(t)\rangle \\ &\quad + \langle w(t), \phi_{m',n',\tau,\nu}(t)\rangle\,. \end{aligned} \tag{14}$$

The computation of the elements of the $\mathbf{Y}_{\rm FT}$ matrix as per (14) needs the computation of the inner products $\langle \phi_{m,n,\tau_i,\nu_i}(t), \phi_{m',n',\tau,\nu}(t)\rangle$. For this, we derive an analytical expression for the inner product between any two orthonormal functions $\phi_{m_1,n_1,\tau_1,\nu_1}(t)$ and $\phi_{m_2,n_2,\tau_2,\nu_2}(t)$, denoted by $\langle \phi_{m_1,n_1,\tau_1,\nu_1}(t), \phi_{m_2,n_2,\tau_2,\nu_2}(t)\rangle$, which is given in the Proposition 1 below (proof is omitted here due to page limit).

Proposition 1. *When $g(t)$ is a rectangular pulse of unit energy, i.e., $g(t) = \frac{1}{\sqrt{T}}\mathbb{1}_{\{0\le t<T\}}$, the inner product $\langle \phi_{m_1,n_1,\tau_1,\nu_1}(t), \phi_{m_2,n_2,\tau_2,\nu_2}(t)\rangle$ is given by (15) given at the bottom of this page.*

The entries of the FT domain channel matrix $\mathbf{H}_{\rm FT}$ in (11) are given by $\mathbf{H}_{\rm FT}[n'M+m', nM+m] = \sum_{i=1}^{P} h_i \langle \phi_{m,n,\tau_i,\nu_i}(t), \phi_{m',n',\tau,\nu}(t)\rangle$, and the DD domain matrix $\mathbf{H}_{\rm DD}$ can be obtained from $\mathbf{H}_{\rm FT}$ through the relation in (13). Depending on the choice of parameters τ and ν used for the projection, $\mathbf{H}_{\rm DD}$ varies and thus the received signal $\mathbf{y}_{\rm DD}$. Different choices of τ and ν gives rise to different receivers. In the conventional receiver, $\{\phi_{m',n',\tau,\nu}(t)\}$ with $\tau=\nu=0$ are the set of orthonormal functions used for the projection, i.e., the same set of functions that are used for transmission. The set of orthonormal functions used for transmission in (4) is different from any of the P sets of orthonormal functions (each set corresponding to a propagation path) present in the received signal in (9), and, as a consequence, the DD domain received signal matrix $\mathbf{Y}_{\rm DD}$ is distorted, influencing the detection performance. The effect of interference caused by this loss of orthogonality in the projection in conventional receiver is mitigated by the proposed receivers presented in the following subsection.

A. Proposed receivers based on DD channel projection

The idea is to restore the transmitted TF domain signals without much distortion at the receiver through the use of better orthonormal functions for projection using channel knowledge. Two receivers are proposed. The first proposed receiver uses projection functions that are obtained based on an approximate characterization of the multipath channel as a channel with a single *effective path*, and the received signal is projected onto this effective path. A cost function is defined for this purpose, which is maximized to obtain the effective path. The idea is obtain the effective path in such a way to make the DD channel matrix close to the identity matrix, which is the ideal desired channel matrix. We call this receiver as the effective path (EP) receiver. For a single-path channel (i.e., $P=1$), the EP receiver turns out to be the optimum receiver. For channels with $P>1$, the EP receiver is shown to outperform the conventional receiver. In the second proposed receiver, the received signal is projected onto N_p paths, $1\le N_p\le P$, and the resulting projected signals are concatenated to obtain the overall DD channel matrix. We call this receiver as the *concatenated paths (CP)* receiver. The idea is that the use of multiple paths for the projection gives complementary views of the same underlying signal that allows better performance. The CP receiver is found to outperform both the conventional as well as the EP receiver.

1) Proposed EP receiver: For every (τ,ν) tuple, we have a set of MN orthonormal functions $\{\phi_{m,n,\tau,\nu}(t), m=0,\cdots,M-1, n=0,\cdots,N-1\}$ that can be used for projecting $y(t)$. For each of these sets, the DD domain channel matrix $\mathbf{H}_{\rm DD}$ is different because the elements in $\mathbf{H}_{\rm FT}$ are dependent on $\phi_{m,n,\tau,\nu}(t)$, and the interference among received data symbols is dependent on $\mathbf{H}_{\rm DD}$. In order to reduce interference, we seek to identify a (τ,ν)-tuple that yields a DD channel matrix that looks more like an identity matrix (which is the desired channel matrix ideally without any interference) when projected onto it. The corresponding (τ,ν) values define what we term the *effective path*. Since we desire $\mathbf{H}_{\rm DD}$ to be as similar to the identity matrix as possible, one cost function that measures the similarity between them is the correlation value between their corresponding vectorized components, i.e., $|\langle \mathbf{h}_{\rm DD}, \mathbf{i}\rangle|$, where $\mathbf{h}_{\rm DD} = {\rm vec}(\mathbf{H}_{\rm DD})$ and $\mathbf{i} = {\rm vec}(\mathbf{I}_{MN})$, and the effective path can be obtained as $(\tau_{\rm eff},\nu_{\rm eff}) = \arg\max_{(\tau,\nu)} \left|\left\langle \mathbf{h}_{\rm DD}^{(\tau,\nu)}, \mathbf{i}\right\rangle\right|$, where $\mathbf{h}_{\rm DD}^{(\tau,\nu)} = {\rm vec}(\mathbf{H}_{\rm DD}^{(\tau,\nu)})$ and $\mathbf{H}_{\rm DD}^{(\tau,\nu)}$ is the channel matrix when τ and ν are used for the projection. Since $\mathbf{H}_{\rm DD}$ and $\mathbf{H}_{\rm FT}$ are similar matrices [12] and trace is preserved, the above cost

$$\begin{aligned}\langle \phi_{m_1,n_1,\tau_1,\nu_1}(t), \phi_{m_2,n_2,\tau_2,\nu_2}(t)\rangle \;=\; & e^{-j2\pi m_1\frac{\Delta\tau}{T}} e^{-j2\pi\nu_1\Delta\tau}\mathbb{1}_{\{\Delta\tau\ge 0\}}\Bigg\{\mathbb{1}_{\{\Delta n=0\}} e^{j2\pi n_1\frac{\Delta\nu}{\Delta f}} e^{j\pi\left(\Delta m+\frac{\Delta\nu}{\Delta f}\right)\left(1+\frac{\Delta\tau}{T}\right)} \\ & \left(1-\frac{\Delta\tau}{T}\right){\rm sinc}\left(\left(\Delta m+\frac{\Delta\nu}{\Delta f}\right)\left(1-\frac{\Delta\tau}{T}\right)\right) + \mathbb{1}_{\{\Delta n=-1\}} e^{j2\pi(n_1+1)\frac{\Delta\nu}{\Delta f}} e^{j\pi\left(\Delta m+\frac{\Delta\nu}{\Delta f}\right)\frac{\Delta\tau}{T}} \\ & \frac{\Delta\tau}{T}{\rm sinc}\left(\left(\Delta m+\frac{\Delta\nu}{\Delta f}\right)\frac{\Delta\tau}{T}\right)\Bigg\} + e^{-j2\pi m_1\frac{\Delta\tau}{T}} e^{-j2\pi\nu_1\Delta\tau}\mathbb{1}_{\{\Delta\tau<0\}}\Bigg\{\mathbb{1}_{\{\Delta n=0\}} e^{j2\pi n_1\frac{\Delta\nu}{\Delta f}} e^{j\pi\left(\Delta m+\frac{\Delta\nu}{\Delta f}\right)\left(1+\frac{\Delta\tau}{T}\right)} \\ & \left(1+\frac{\Delta\tau}{T}\right){\rm sinc}\left(\left(\Delta m+\frac{\Delta\nu}{\Delta f}\right)\left(1+\frac{\Delta\tau}{T}\right)\right) - \mathbb{1}_{\{\Delta n=1\}} e^{j2\pi n_1\frac{\Delta\nu}{\Delta f}} e^{j\pi\left(\Delta m+\frac{\Delta\nu}{\Delta f}\right)\frac{\Delta\tau}{T}}\frac{\Delta\tau}{T}{\rm sinc}\left(\left(\Delta m+\frac{\Delta\nu}{\Delta f}\right)\left(\frac{\Delta\tau}{T}\right)\right)\Bigg\}, \end{aligned} \tag{15}$$

where $\Delta\tau=\tau_1-\tau_2$, $\Delta\nu=\nu_1-\nu_2$, $\Delta m=m_1-m_2$, and $\Delta n=n_1-n_2$.

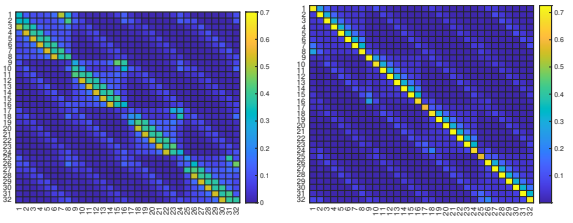

(a) Conventional Rx projection (b) Proposed EP Rx projection

Figure 1: Heat maps of the $\mathbf{H}_{\text{DD}}$ matrices for $P = 3$ paths, (a) for conventional receiver with projection using $\{\phi_{m,n,0,0}(t)\}$ and (b) for proposed EP receiver with projection using $\{\phi_{m,n,\hat{\tau}_{\text{eff}},\hat{\nu}_{\text{eff}}}(t)\}$.

function can be written as

$$\left|\left\langle \mathbf{h}_{\text{DD}}^{(\tau,\nu)}, \mathbf{i} \right\rangle\right| = \left|\text{Tr}(\mathbf{H}_{\text{DD}}^{(\tau,\nu)})\right| = \left|\text{Tr}(\mathbf{H}_{\text{FT}}^{(\tau,\nu)})\right| = \left|\sum_{i=1}^{P} h_i' \mathbf{1}_N^H \mathbf{b}_N^{(i)} {\mathbf{a}_M^{(i)}}^H \mathbf{1}_M\right|, \quad (16)$$

where $h_i' = h_i e^{-j2\pi\nu_i(\tau_i-\tau)} e^{j\pi\left(\frac{\nu_i-\nu}{\Delta f}\right)\left(1-\frac{\tau_i-\tau}{T}\right)} \left(1-\left|\frac{\tau_i-\tau}{T}\right|\right)\times \text{sinc}\left(\left(\frac{\nu_i-\nu}{\Delta f}\right)\left(1-\left|\frac{\tau_i-\tau}{T}\right|\right)\right)$, $\mathbf{1}_M$ is a vector of length M with all ones, $\mathbf{a}_M^{(i)} \in \mathbb{C}^{M\times 1}$ with $\mathbf{a}_M^{(i)}[m] = e^{-j2\pi m\left(\frac{\tau_i-\tau}{T}\right)}$, and $\mathbf{b}_N^{(i)} \in \mathbb{C}^{N\times 1}$ with $\mathbf{b}_N^{(i)}[n] = e^{j2\pi n\left(\frac{\nu_i-\nu}{\Delta f}\right)}$. To find $(\tau_{\text{eff}}, \nu_{\text{eff}})$, we employ a two step procedure. In the first step, we find the on-grid component of $(\tau_{\text{eff}}, \nu_{\text{eff}})$. In the second step, we find the off-grid component around the on-grid component obtained from the first step. The search space in the first step is $\left\{\left(\frac{l}{M\Delta f}, \frac{k}{NT}\right) : l \in \{0,\cdots,l_{\max}\}, k \in \{-k_{\max},\cdots,k_{\max}\}\right\}$, where $l_{\max} = \lceil \tau_{\max} M\Delta f \rceil$, $k_{\max} = \lceil \nu_{\max} NT \rceil$, and $(\tau_{\max}, \nu_{\max})$ are the maximum delay and Doppler of the channel.

The algorithm for finding the off-grid component (around the on-grid component $(\tilde{\tau}_{\text{eff}}, \tilde{\nu}_{\text{eff}})$) The algorithm is an iterative one, where the search space gets refined with each iteration. The effective path $(\hat{\tau}_{\text{eff}}, \hat{\nu}_{\text{eff}})$ obtained from **Algorithm 1** is used for projecting $y(t)$ onto the functions $\{\phi_{m,n,\hat{\tau}_{\text{eff}},\hat{\nu}_{\text{eff}}}(t)\}$ to get the FT signal and subsequently the corresponding DD domain signal on which detection of symbols is carried out.

The effectiveness of the projection in the proposed EP receiver compared to that in the conventional receiver is illustrated in Fig. 1 which shows the heat maps of their corresponding $\mathbf{H}_{\text{DD}}$ matrices. While the conventional receiver uses the functions $\{\phi_{m,n,0,0}(t)\}$ for projection, the EP receiver uses $\{\phi_{m,n,\hat{\tau}_{\text{eff}},\hat{\nu}_{\text{eff}}}(t)\}$ for projection. It can be seen that the diagonal elements of the $\mathbf{H}_{\text{DD}}$ matrix in the EP receiver are more dominant (compared to the off-diagonal interference terms) compared to that in the conventional receiver, which is what the proposed projection is intended to achieve. This interference suppression ability of the EP receiver, in turn, leads to better bit error performance (as will be shown in the results and discussion in Sec. IV).

2) Proposed CP receiver: In the EP receiver, there can be unsuppressed residual interference despite the projection of

Algorithm 1 Finding off-grid component of $(\tau_{\text{eff}}, \nu_{\text{eff}})$

Inputs: h_is, τ_is, ν_is, on-grid component $(\tilde{\tau}_{\text{eff}}, \tilde{\nu}_{\text{eff}})$, $s_{\max}$
Initialize: $s = 1, \hat{\tau}_{\text{eff}}^{(0)} = \tilde{\tau}_{\text{eff}}, \hat{\nu}_{\text{eff}}^{(0)} = \tilde{\nu}_{\text{eff}}$
repeat
Search space:

$$\Gamma = \left(\left\{\frac{\hat{\tau}_{\text{eff}}^{(s-1)} M\Delta f - 5\cdot 10^{-s}}{M\Delta f}, \frac{\hat{\tau}_{\text{eff}}^{(s-1)} M\Delta f - 4\cdot 10^{-s}}{M\Delta f}, \cdots, \frac{\hat{\tau}_{\text{eff}}^{(s-1)} M\Delta f + 5\cdot 10^{-s}}{M\Delta f}\right\} \times \left\{\frac{\hat{\nu}_{\text{eff}}^{(s-1)} NT - 5\cdot 10^{-s}}{NT}, \frac{\hat{\nu}_{\text{eff}}^{(s-1)} NT - 4\cdot 10^{-s}}{NT}, \cdots, \frac{\hat{\nu}_{\text{eff}}^{(s-1)} NT + 5\cdot 10^{-s}}{NT}\right\}\right)$$

$$\left(\hat{\tau}_{\text{eff}}^{(s)}, \hat{\nu}_{\text{eff}}^{(s)}\right) = \arg\max_{(\tau,\nu)\in\Gamma} \left|\left\langle \mathbf{h}_{\text{DD}}^{(\tau,\nu)}, \mathbf{i} \right\rangle\right|$$

Update $s = s + 1$
Until $s = s_{\max}$
Output: $(\hat{\tau}_{\text{eff}}, \hat{\nu}_{\text{eff}}) = \left(\hat{\tau}_{\text{eff}}^{(s_{\max})}, \hat{\nu}_{\text{eff}}^{(s_{\max})}\right)$

$y(t)$ onto the effective path to suppress interference. Also, if the received signal is projected onto any one path among the P paths, there will be residual interference. This is because, by projecting $y(t)$ onto (τ_i, ν_i), the $\mathbf{H}_{\text{DD}}^{(i)}$ matrix can be made an identity matrix but not the $\mathbf{H}_{\text{DD}}^{(j)}$, $j \neq i$ matrices, and therefore the overall channel matrix $\mathbf{H}_{\text{DD}} = \sum_{i=1}^{P} h_i \mathbf{H}_{\text{DD}}^{(i)}$ will not be an identity matrix. Since the projection onto any particular path does not suppress the interference from other paths, we propose to use multiple paths for the projection, potentially getting complementary views of the same underlying signal and use these projections for obtaining the signal for detection.

Towards this, we select N_p paths from the P available paths, $1 \leq N_p \leq P$, and use these N_p paths for projection purposes. These N_p paths are taken to be the paths with the strongest channel coefficients. Using the selected N_p paths, we obtain the set of projections $\left\{\mathbf{y}_{\text{DD}}^{(\tau_{c_i},\nu_{c_i})}\right\}_{i=1}^{N_p}$, where c_i denotes the ith chosen path, (τ_{c_i},ν_{c_i}) denotes the delay and Doppler of the ith chosen path, and $\mathbf{y}_{\text{DD}}^{(\tau_{c_i},\nu_{c_i})}$ denotes the received signal when $y(t)$ is projected on to the ith chosen path. Every element of this set of projections, say $\mathbf{y}_{\text{DD}}^{(\tau_{c_i},\nu_{c_i})}$, is the sum of transmitted signal scaled by a factor h_{c_i} (because the signal on c_ith path is received properly) and the interference from other paths. This set of projections of $y(t)$ onto N_p paths is used for detection by forming a concatenated received signal vector $\mathbf{y}'_{\text{DD}} \in \mathbb{C}^{N_p MN\times 1}$ using these projections as

$$\mathbf{y}'_{\text{DD}} = \begin{bmatrix} \mathbf{y}_{\text{DD}}^{(\tau_{c_1},\nu_{c_1})} \\ \vdots \\ \mathbf{y}_{\text{DD}}^{(\tau_{c_{N_p}},\nu_{c_{N_p}})} \end{bmatrix} = \mathbf{H}'_{\text{DD}}\mathbf{x}_{\text{DD}} + \mathbf{w}', \quad (17)$$

where $\mathbf{H}'_{\text{DD}} = \begin{bmatrix} \mathbf{H}_{\text{DD}}^{(\tau_{c_1},\nu_{c_1})} \\ \vdots \\ \mathbf{H}_{\text{DD}}^{(\tau_{c_{N_p}},\nu_{c_{N_p}})} \end{bmatrix}$ and $\mathbf{w}' = \begin{bmatrix} \mathbf{w}_1 \\ \vdots \\ \mathbf{w}_{N_p} \end{bmatrix}$.

The $\mathbf{H}_{\text{DD}}^{(\tau_{c_i},\nu_{c_i})} \in \mathbb{C}^{MN\times MN}$ matrix and $\mathbf{w}_i \in \mathbb{C}^{MN\times 1}$ vector denote the channel matrix and noise vector, respec-

tively, when $y(t)$ is projected onto the ith chosen path. The concatenated system model given by (17) serves as the basis for subsequent signal detection. The number of paths chosen for projection impacts the detection performance. While using all paths ($N_p = P$) offers the best performance, projecting onto a lesser number of strongest paths ($N_p < P$) provides complexity advantage at the cost of performance, providing a tradeoff between complexity and performance.

Noise statistics: Unlike the components of noise in (13), the components of noise in (17) are not i.i.d. Gaussian, i.e., $\mathbf{w}' \sim \mathcal{CN}(0, \mathbf{R}_{ww}), \mathbf{R}_{ww} \neq \alpha \mathbf{I}_{N_p MN}$, because the $N_p MN$ functions which are used for obtaining the components of $\mathbf{w}'$ are non-orthogonal to each other. The expression for the covariance matrix $\mathbf{R}_{ww}$ is derived in Appendix A.

IV. Results and Discussions

In this section, we present the simulation results on the bit error rate (BER) performance of the proposed EP and CP receivers in comparison with that of the conventional receiver. MMSE and MMSE-SoftIC (MMSE with soft interference cancellation) detection with perfect channel state information (CSI) and estimated CSI are considered. Two OTFS systems with $(M = 32, N = 16)$ and $(M = 8, N = 4)$ are considered. The subcarrier spacing Δf is set to 30 kHz. The channel is modeled with $P = 5$ propagation paths. The path delays are uniformly distributed in the range $[0, 7\mu s]$. Doppler shift for the pth path is generated using Jake's Doppler spectrum according to the equation $\nu_p = \nu_{\max} \cos(\theta_p)$, where θ_p is uniformly distributed in $(0, 2\pi]$ and $\nu_{\max}$ is 1700 Hz.

Figure 2 depicts the BER performance of the proposed EP and CP receivers for $M = 32$, $N = 16$, 4-QAM and perfect CSI. The performance of the conventional receiver is also shown. Uniform power delay profile (PDP) is employed to generate the channel coefficients for each path. All receivers utilize linear MMSE equalizer followed by minimum distance decoding for signal detection. The proposed EP receiver that leverages the 'effective path' for projection achieves an SNR improvement of about 1.5 dB at 10^{-4} BER compared to the conventional receiver. This improvement can be attributed to the resulting channel exhibiting a higher correlation with the identity matrix, as shown in Fig. 1. This reduces the DD domain inter-symbol interference, resulting in better performance compared to the conventional receiver. Further, the proposed CP receiver with $N_p = P$ performs even better, i.e., the CP receiver outperforms the conventional receiver by about 2.5 dB at 10^{-4} BER. This advantage arises from the CP receiver receiving the signal along with interference from other paths in an almost unperturbed manner for each projection. Additionally, the CP receiver utilizes P such views of the signal for improved detection.

The effect of varying the number of concatenated paths N_p in the proposed CP receiver for $M = 32$, $N = 16$, 16-QAM, perfect CSI, and MMSE detection is depicted in Fig. 3. N_p is chosen for projection based on the path energy, prioritizing paths with stronger coefficients. As can be observed, the

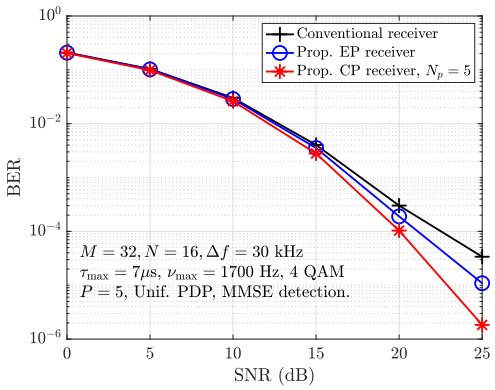

Figure 2: BER vs SNR performance of the proposed EP and CP receivers with MMSE detection.

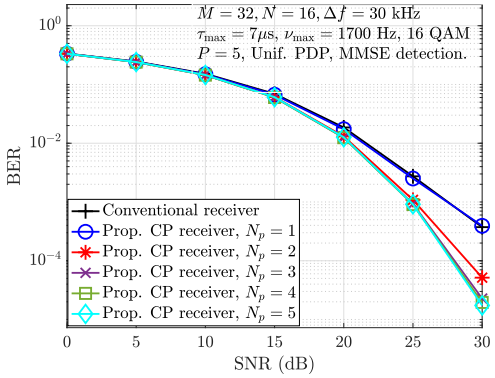

Figure 3: BER vs SNR performance of the proposed CP receiver for different number of concatenated paths N_p with MMSE detection.

performance is dependent on the number of paths incorporated into the projection. When $N_p = 1$, the CP receiver's performance aligns with that of the conventional receiver. This is attributed to the fact that with a single path used for projection, the CP receiver effectively replicates the behavior of the conventional receiver. As the number of projections is incremented, a continuous improvement in performance is observed. This enhancement is particularly pronounced when N_p is initially increased. This can be attributed to the inclusion of additional unperturbed views of the signal in each projection, incorporating stronger paths with dominant signal information. These stronger paths significantly contribute to the receiver's ability to detect the data correctly. However, further increments in N_p yield diminishing returns. This is because progressively weaker paths contribute less significant information to the overall signal.

Figure 4 presents the BER performance of all the three receivers for $M = 8$, $N = 4$, and 4-QAM, with MMSE and MMSE-SoftIC detection. The maximum number of iterations used in the MMSE-SoftIC algorithm is 4. As can be observed, all the receivers show improved performance with MMSE-SoftIC detection compared to that with MMSE detection, but the amount of improvement due to MMSE-SoftIC varies across the receivers. The conventional receiver exhibits the

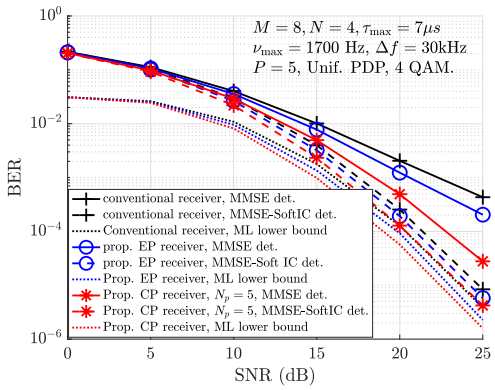

Figure 4: BER vs SNR performance of the different receivers using MMSE and MMSE-SoftIC detection in comparison with lower bound on optimum maximum likelihood performance.

highest improvement with MMSE-SoftIC detection compared to MMSE detection. This can be attributed to the fact that there is significant unmitigated interference among data symbols in the conventional receiver. The iterative cancellation process effectively mitigates this interference, leading to a more pronounced performance improvement. The EP receiver shows a relatively smaller improvement due to MMSE-SoftIC detection. This can be explained by the fact that the EP receiver inherently reduces the impact of interference by projection on the effective path, leaving lesser room for improvement. The CP receiver exhibits the smallest improvement with MMSE-SoftIC detection among the three receivers. This behavior can be understood by considering that the CP receiver already leverages projections of the signal onto multiple paths, which helps to mitigate the interference significantly. Therefore, the additional benefit gained from iterative cancellation is less pronounced compared to the other receivers. The figure also shows the performance of the detectors in terms of nearness to a lower bound on the optimum maximum likelihood (ML) detection. It can be observed that all the receivers with MMSE-SoftIC detection achieve close to their respective ML lower bounds within about 1 to 2 dB at high SNRs, illustrating the effectiveness of the proposed projection receivers and iterative detection.

V. Conclusions

We proposed two receivers for OTFS which are aimed at mitigation of interference across information symbols due to DD channel spreads. The receivers are based on the use of projections that exploit DD channel knowledge for transforming the received time domain signal to FT domain that reduced interference. The proposed EP receiver identified an optimal effective path that renders the effective channel matrix to be close to an identity matrix and the received signal is projected onto this effective path. The proposed CP receiver projected the received signal onto a chosen subset of the channel paths, providing multiple views of the underlying data symbols, which are then combined for improved detection performance. The proposed receivers outperformed the conventional OTFS receiver due to their superior interference mitigation ability. Future work can consider enhancement of the proposed receivers, e.g., taking DD channel estimation into account.

Appendix A
Noise statistics of the proposed CP receiver

Consider the FT domain noise $\tilde{\mathbf{w}}'$ of the proposed CP receiver, $\tilde{\mathbf{w}}' = \begin{bmatrix} \tilde{\mathbf{w}}_1 \\ \vdots \\ \tilde{\mathbf{w}}_{N_P} \end{bmatrix} \in \mathbb{C}^{N_p MN \times 1}$, where $\tilde{\mathbf{w}}_i = \text{vec}(\mathbf{W}_i)$ and $\mathbf{W}_i[m,n] = \int w(t)\phi_{m,n,\tau_i,\nu_i}(t)\ dt$. Since the components of $\tilde{\mathbf{w}}'$ are linear functionals of $\{\phi_{m,n,\tau_i,\nu_i}(t)\}$, $i = 1, \cdots, N_p$, the components of $\tilde{\mathbf{w}}_c$ are jointly Gaussian [13]. Hence, it suffices to know its mean and covariance to describe the distribution of $\tilde{\mathbf{w}}_c$. Consider the components $\tilde{w}_k = \langle w(t), \phi_{m_1,n_1,\tau_i,\nu_i}(t)\rangle$, and $\tilde{w}_l = \langle w(t), \phi_{m_2,n_2,\tau_j,\nu_j}(t)\rangle$ of $\tilde{\mathbf{w}}_c$. The mean of $\tilde{w}_k$ is $\mathbb{E}[\tilde{w}_k] = \mathbb{E}[\langle w(t), \phi_{m_1,n_1,\tau_i,\nu_i}(t)\rangle] = 0$. The variance between $\tilde{w}_k$ and $\tilde{w}_l$ can be obtained as $\mathbb{E}\left[\tilde{w}_k \tilde{w}_l^H\right] = \sigma^2 \langle \phi_{m_2,n_2,\tau_j,\nu_j}(t), \phi_{m_1,n_1,\tau_i,\nu_i}(t)\rangle$. The covariance matrix of $\tilde{\mathbf{w}}'$ can be written as $\tilde{\mathbf{R}} = \begin{bmatrix} \tilde{\mathbf{R}}_{11} & \cdots & \tilde{\mathbf{R}}_{1N_p} \\ \vdots & \ddots & \vdots \\ \tilde{\mathbf{R}}_{N_p 1} & \cdots & \tilde{\mathbf{R}}_{N_p N_p} \end{bmatrix}$, where $\tilde{\mathbf{R}}_{kl} \in \mathbb{C}^{MN \times MN}$ whose (i,j)th element is $\langle \phi_{m_2,n_2,\tau_l,\nu_l}(t), \phi_{m_1,n_1,\tau_k,\nu_k}(t)\rangle$. Here, $i = n_1 M + m_1, j = n_2 M + m_2$ and $i, j \in \{0, 1, \cdots, MN-1\}, m_1, m_2 \in \{0, 1, \cdots, M-1\}, n_1, n_2 \in \{0, 1, \cdots, N-1\}$. Now, the DD domain noise $\mathbf{w}'$ can be written as $\mathbf{w}' = \mathcal{F}\tilde{\mathbf{w}}'$, where $\mathcal{F} = \text{diag}\{\mathcal{F}_1, \cdots, \mathcal{F}_{N_P}\}$, $\mathcal{F}_i = \mathbf{F}_N \otimes \mathbf{F}_M^H\ \forall i$ (since $\mathbf{w}_i = (\mathbf{F}_N \otimes \mathbf{F}_M^H)\tilde{\mathbf{w}}_i$). Therefore, the covariance matrix of $\mathbf{w}_c$, $\mathbf{R}$ is given by $\mathbf{R} = \mathbb{E}\left[\mathbf{w}'\mathbf{w}'^H\right] = \mathbb{E}\left[\mathcal{F}\tilde{\mathbf{w}}'\tilde{\mathbf{w}}'^H\mathcal{F}^H\right] = \mathcal{F}\tilde{\mathbf{R}}\mathcal{F}^H$.

References

[1] R. Hadani et al., "Orthogonal time frequency space modulation," *Proc. IEEE WCNC'2017*, pp. 1-6, Mar. 2017.

[2] Z. Wei et al., "Orthogonal time-frequency space modulation: a promising next-generation waveform," *IEEE Wireless Commun. Mag.*, vol. 28, no. 4, pp. 136-144, Aug. 2021.

[3] Y. Hong, T. Thaj, and E. Viterbo, *Delay-Doppler Communications: Principles and Applications*, London UK: Elsevier, 2022.

[4] P. Raviteja, K. T. Phan, Y. Hong, and E. Viterbo, "Interference cancellation and iterative detection for orthogonal time frequency space modulation," *IEEE Trans. Wireless Commun.*, pp. 6501-6515, Aug. 2018.

[5] M. K. Ramachandran and A. Chockalingam, "MIMO-OTFS in high-Doppler fading channels: signal detection and channel estimation," *Proc. IEEE GLOBECOM'2018*, pp. 206-212, Dec. 2018.

[6] W. Yuan, Z. Wei, J. Yuan, and D. W. K. Ng, "A simple variational Bayes detector for orthogonal time frequency space (OTFS) modulation," *IEEE Trans. Veh. Tech.*, vol. 69, no. 7, pp. 7976-7980, Jul. 2020.

[7] L. Xiang, Y. Liu, L-L. Yang, and L. Hanzo, "Gaussian approximate message passing detection of orthogonal time frequency space modulation," *IEEE Trans. Veh. Tech.*, vol. 70, no. 10, pp. 10999-11004, Oct. 2021.

[8] L. Zhao, W. J. Gao, and W. Guo, "Sparse Bayesian learning of delay-Doppler channel for OTFS system," *IEEE Commun. Lett.*, vol. 24, no. 12, pp. 2766-2769, Dec. 2020.

[9] Z. Wei, W. Yuan, S. Li, J. Yuan, and D. W. K. Ng, "Off-grid channel estimation with sparse Bayesian learning for OTFS systems," *IEEE Trans. Wireless Commun.*, vol. 21, no. 9, pp. 7407-7426, Sep. 2022.

[10] I. A. Khan and S. K. Mohammed, "A low-complexity OTFS channel estimation method for fractional delay-Doppler scenarios," *IEEE Wireless Commun. Lett.*, vol. 12, no. 9, pp. 1484-1488, Sep. 2023.

[11] K. B. Petersen and M. S. Pedersen, *The Matrix Cookbook*, Techn. Univ. Denmark, Nov. 2012.

[12] R. Horn and C. Johnson, *Matrix Analysis*, Cambridge Univ. Press, 2013.

[13] R. G. Gallager, *Principles of Digital Communication*, Cambridge Univ. Press, 2008.